Metastable H+ 3 formation and decay in the reaction of highly excited H+ 2 with H2

Jay K. Badenhoop, George C. Schatz, and Charles W. Eaker

Citation: The Journal of Chemical Physics **87**, 5317 (1987); doi: 10.1063/1.453649
View online: http://dx.doi.org/10.1063/1.453649
View Table of Contents: http://scitation.aip.org/content/aip/journal/jcp/87/9?ver=pdfcov
Published by the AIP Publishing

Metastable H_3^+ formation and decay in the reaction of highly excited H_2^+ with H_2

Jay K. Badenhoop and George C. Schatz
Department of Chemistry, Northwestern University, Evanston, Illinois 60201
Charles W. Eaker
Department of Chemistry, University of Dallas, Irving, Texas 75061

(Received 15 May 1987; accepted 28 July 1987)

This paper presents the detailed results of a quasiclassical trajectory surface hopping study of reaction of highly vibrationally excited H_2^+ with ground state H_2 (and isotopic counterparts $H_2^+ + D_2$, $D_2^+ + H_2$, and $D_2^+ + D_2$), with particular emphasis on the formation and decay of metastable H_3^+ products. A diatomics-in-molecules surface is used which has been successful in previous studies of $H_2^+(v) + H_2$ at low v. In the present study, we consider $v = 0$–17, and find that metastable H_3^+'s are a major product for $v \geqslant 13$. Some of these metastables decay rapidly, showing exponential lifetime distributions with 2–7 ps lifetimes depending on v and on isotope. The remaining H_3^+'s have much longer lifetimes, and a number of methods are used to determine the origin of their stability. In no cases are any of these molecules found to be quasiperiodic, but a Fourier spectral analysis reveals some decoupling of H^+–H_2 orbital motion from H_2 rotational motion, and we find that many molecules have long lifetimes even though they have energies which are above any rigorous centrifugal barrier. The relation of these results to recent infrared absorption measurements on highly excited H_3^+'s is discussed.

I. INTRODUCTION

The reaction

$$H_2^+ + H_2 \rightarrow H_3^+ + H \tag{1}$$

has been of fundamental importance ever since it was discovered in early ion–molecule work,[1] and as a result it has been the subject of numerous experimental[1,2] and theoretical studies.[3–5] Recently, measurements by Carrington and Kennedy[6] have provided information about the H_3^+ product of this reaction that presents a new and significant challenge to understanding the dynamics of this reaction. In their measurements, infrared absorption was used to observe highly excited states of H_3^+ that are produced following electron bombardment of H_2 gas. Reaction (1) was implicated as being the major contributor to the production of these H_3^+ ions. Since absorption of radiation was detected by monitoring H^+ produced following photodissociation, only H_3^+ states which could be dissociated upon absorption of one photon ($\hbar\omega = 800$–$1000\ \mathrm{cm}^{-1}$) were observed. However it was found that the spectrum of such states is extremely rich (27 000 lines were observed!). In addition many long-lived states (10^{-7}–10^{-9} s) were found above the threshold for dissociation. This threshold occurs at 4.7 eV internal energy in H_3^+ and even though reaction (1) is exoergic by 1.9 eV, 2.8 eV of reagent energy (translational, rotational, vibrational) is required to produce the observed H_3^+'s. Since the translational and rotational motions of the reagents are expected to be largely thermal in the source used, this energy must come from vibrational excitation. Although the H_2^+ produced by electron bombardment can be sufficiently vibrationally excited to produce H_3^+ above its dissociation threshold, the states of H_2^+ which are actually required to produce highly excited H_3^+ depends on how reagent energy is partitioned to the products of reaction (1). Quite a bit is known about this partitioning for the lower states of H_2^+ ($v = 0$–3, especially[5]), but the analogous information for highly excited H_2^+ has not been studied. In addition, two key questions that arise from the Carrington and Kennedy measurements are: (1) what states of H_3^+ are responsible for the observed spectra? and (2) what is the mechanism responsible for the existence of the long-lived metastable H_3^+?

In this paper we present the results of a quasiclassical trajectory study which is designed to address these questions through an analysis of the products of reaction (1) when the H_2^+ reagent is highly excited. Our motivation in this work is not to assign all the lines in the spectrum, but rather to learn at a qualitative level what kinds of H_3^+ motions are present and what dynamical information might be extracted from the measured spectra.

In addition to reaction (1), we also consider the isotopic counterparts:

$$D_2^+ + D_2 \rightarrow D_3^+ + D, \tag{2}$$

$$H_2^+ + D_2 \rightarrow D_2H^+ + H \tag{3a}$$

$$\rightarrow DH_2^+ + D, \tag{3b}$$

$$D_2^+ + H_2 \rightarrow D_2H^+ + H \tag{4a}$$

$$\rightarrow DH_2^+ + D. \tag{4b}$$

One of the surprising results of Ref. 6 was that the spectra of D_2H^+ measured by monitoring H^+ were different than those taken monitoring D^+. We will use our results for reactions (2)–(4) to study this and other isotope effects.

The method used for these studies is the quasiclassical trajectory method, augmented by a trajectory surface hopping (TSH) algorithm[5(a),7] to include for the several potential surfaces involved. The TSH method has been used in several earlier studies of $H_2^+ + H_2$[5(a),5(b),5(e)] in conjunction

 0021-9606/87/215317-08$02.10

with diatomics-in-molecules (DIM) potential surfaces, and the results of these calculations have been in good agreement with experiments.

Preliminary results of the present application to highly excited states of H_2^+ have recently been presented.[8] In that paper we examined the dependence of the H_3^+ internal energy distribution on initial H_2^+ vibrational state (for a translational energy of 0.5 eV) and we found that significant population of H_3^+ at and above its dissociation energy occurs for $v \geqslant 13$. Two different parametrizations of the H_4^+ DIM potential surface were considered to see if the results showed much variation. Since they did not, we have only considered one potential surface in the calculations which are reported here.

One earlier study that is relevant to the present work is that by Child[9] who attempted to characterize predissociative orbiting states of H_3^+ that were postulated by Carrington and Kennedy to be responsible for many of the more important lines in their spectra. Child used a restricted basis set quantum mechanical scattering analysis to study these H^+–H_2 states, and he found that the longest lived of these states are bound behind centrifugal barriers associated with the H^+–H_2 orbital motion.

Subsequent to this, Pollak[10] noted that (based on the earlier work of Ref. 11) there are rigorously defined centrifugal barriers to H_3^+ dissociation that could be responsible for the existence of long-lived metastables. In particular, Pollak found that metastables were possible for H_3^+ angular momenta up to $J = 70$, with energy up to 1 eV above dissociation. In neither the Child nor Pollak studies was the question of H_3^+ formation addressed so it is not known whether reactions which produce H_3^+ with such high rotational angular momenta actually occur. We will consider this point in this paper.

II. DESCRIPTION OF CALCULATIONS

Collisions of H_2^+ with H_2 were studied using the trajectory surface hopping method of Ref. 5(a) in conjunction with the standard quasiclassical sampling of initial conditions. The potential surface used is that of Polak,[4(a)] and it is characterized by a reaction exoergicity of 2.13 eV, and an H_3^+ dissociation energy (to $H_2 + H^+$) of 4.92 eV. These energies are both high by 0.2 eV compared to the experimental results quoted in the Introduction. At the collision energies of interest, although it is possible to excite H_3^+ electronically, none of the trajectories integrated actually led to excited H_3^+ even though the lowest excited state was explicitly included in the calculation. The selection of initial condition parameters (initial diatomic states) is largely the same as is described in Ref. 5(c), but because we considered H_2^+ vibrational states as high as $v = 17$, it was necessary to increase the initial diatom–diatom separation (to $16\,a_0$) and the maximum impact parameter (to typically $13\,a_0$) in order to calculate converged cross sections.

The most significant changes in our calculation were made in the analysis of the products. In our earlier work at low v, it had been possible to determine the complete set of good constants of the motion (the good actions) governing the H_3^+ vibrations and rotations.[5(c)] Such calculations were not possible in the present calculations in which H_3^+ has energies close to and above dissociation, as trajectories were always found to be chaotic. We established this both by examining power spectra, and by plotting trajectory motion in a number of different ways, as will be discussed in Sec. III D. Although our original good action analysis was based on evaluating action integrals using phase space contours defined by normal coordinates, we also considered a variety of internal coordinate choices to look for nonchaotic behavior but did not find it.

For H_3^+'s which were produced with energies above the dissociation threshold, it was necessary to further analyze in a variety of ways. First it was important to separate those H_3^+'s which had some existence as a distinct molecule from those which underwent rapid dissociation. To do this, we "aged" the H_3^+'s for 0.36 ps after they were formed, and discarded those that dissociated during this interval. We define the term "*metastable*" to refer to any H_3^+ that survives this long. Since 0.36 ps corresponds to about 15 periods of the lowest frequency mode of H_3^+, this aging period is long enough to discard any H_3^+'s that do not have a structured vibrational spectrum. At the same time, this aging time is over 10 times shorter than the average time needed to dissociate by the majority of metastable molecules.

For those H_3^+'s found to be metastable, we examined lifetime distributions to determine unimolecular decay rates. This requires further integrating the H_3^+'s, and we did this using the ground state H_3^+ surface which can be derived from the H_4^+ surface. Typical trajectory lifetimes were in the 5 ps range, but we found many trajectories which did not undergo dissociation within 30 ps. We will label these nondissociating H_3^+'s as "*quasistable*" (i.e., "seemingly" stable, although probably some of the molecules categorized this way are on the tail end of the 5 ps lifetime distribution). Much of our analysis in Sec. III D will be devoted to determining why quasistable molecules do not dissociate.

One simple model which can be used to diagnose why some trajectories are quasistable and others are not is to examine the rigorous centrifugal barriers[10,11] governing dissociation. To define these barriers, we consider the effective potential associated with dissociation of H_3^+ into $H_2 + H^+$. For a given H_2–H^+ separation R this is obtained by summing the potential energy surface with the centrifugal potential associated with the moment of inertia element perpendicular to the H_3^+ molecular plane, and then minimizing the result with respect to the H_2 internuclear separation and orientation angle. The energy E_b of the barrier found with this effective potential is plotted in Fig. 1 as a function of the H_3^+ angular momentum J for all the possible isotopic variants of H_3^+. This figure shows that the centrifugal barrier increases monotonically with increasing J, with the higher barriers typically being associated with the lighter ions and lighter diatomics. The influence of ion mass is generally more important than diatomic mass in determining barrier height, but it should be noted that dissociation to give an HD diatomic (i.e., $H^+ + HD$, $D^+ + HD$) always leads to barriers that are lower than the corresponding D_2 diatomic bar-

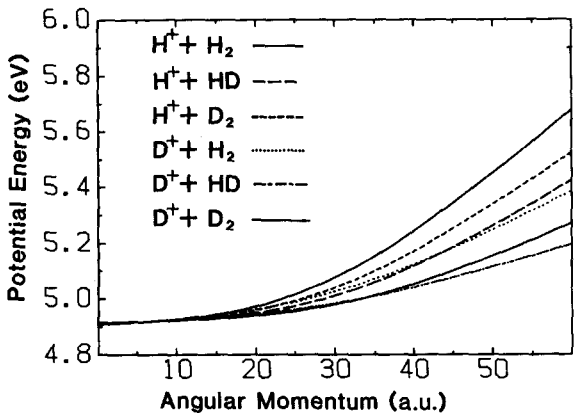

FIG. 1. Energy (eV) vs total rotational angular momentum for the centrifugal barriers associated with dissociation of H_3^+ isotopes: $H^+ + H_2$ (solid, curve at top), $H^+ + HD$ (long dashes), $H^+ + D_2$ (short dashes), $D^+ + H_2$ (dots), $D^+ + HD$ (dash–dot), $D^+ + D_2$ (solid curve near bottom).

riers, irrespective of what ion is involved. This arises because the centrifugal barrier geometry is always linear on the DIM surface, and for HD, the nonsymmetrical center of mass location leads to larger R values and hence smaller centrifugal barriers than for D_2 even though the moment of inertia is smaller. As a result of this, the barrier for dissociation of H_2D^+ into $H^+ + HD$ is below that for $D^+ + H_2$ at high J. Dissociation of D_2H^+, by contrast, has a much higher barrier for forming $H^+ + D_2$ than $D^+ + HD$.

Although the barriers in Fig. 1 provide rigorous bottlenecks to dissociation, it is always possible that dissociation is prevented by even higher barriers that arise from dynamical decoupling of certain degrees of freedom. In Sec. III D we will study the correlation between the internal energy E_{int} and angular momentum of each metastable triatomic and its subsequent dissociation behavior to see if the barriers defined in Fig. 1 serve as the only bottlenecks to dissociation. Further constraints on phase space randomization would show up in the E_{int}–J plot as trajectories that are above all rigorous barriers but do not dissociate.

III. RESULTS

A. Initial state dependence of cross sections

Table I presents the reactive cross sections Q for $H_2^+ + H_2$ as a function of the initial H_2^+ vibrational quantum number v for initial translational energies $E_{tr} = 0.05$ and 0.50 eV. In addition to the cross sections, we also give the average H_3^+ internal energy $\langle E_{int} \rangle$, and angular momentum $\langle J \rangle$ for both stable (S), metastable (M) and total ($T = S + M$) products. Some of the results at 0.50 eV have been calculated previously for the same potential surface,[5(c),5(e)] and the present results are the same within statistical uncertainty.

Table I shows a number of interesting trends. The S cross sections decrease with increasing E_{tr} and they likewise decrease with increasing v, with the decrease more rapid at low E_{tr} and low v. The $v = 0$–3 results have been discussed previously,[5(e)] but note that for $v > 7$ the 0.05 eV S cross sections drop off more slowly with v than the 0.50 eV cross sections. The M cross sections rise monotonically with v starting at $v = 10$, and at $v = 17$ they are substantially larger than the S cross sections. The sum $T = S + M$ has a minimum at $v = 13$ for both energies, and then rises sharply so that it is larger at $v = 17$ than at lower v.

Although it is not simple to explain all of these features, we expect that increase in the charge transfer probability with increasing v plays a major role in suppressing reaction up to $v = 13$. For very large v one runs into the unusual situation that the outer vibrational turning point of the H_2^+ can occur *outside* the H_2^+–H_2 centrifugal barrier, leading to a non-Langevin enhancement in the cross section. It appears that this plays some role in producing the large cross sections for $v = 17$ as the outer turning point occurs at an H–H separation of 10.4 a_0.

The production of metastables at high v is the expected consequence of the increase in the internal energy with v. The variation of $\langle E_{int} \rangle$ with v was studied in detail in Ref. 8 and it was found that the product internal energy actually increases more rapidly with v than the reagent energy, indicating a change in energy partitioning behavior that favors

TABLE I. Cross sections, average product internal energies, and angular momenta for $H_2^+ + H_2$.

		$Q(a_0^2)$			$\langle E_{int}$ (eV)$\rangle$		$\langle J \rangle$	
v	E_{tr} (eV)	Stable (S)	Metastable (M)	Total (T)	Stable (S)	Metastable (M)	Stable (S)	Metastable (M)
0	0.05	363 ± 20	0	363 ± 20	1.90	···	11	···
3		320 ± 27	0	320 ± 27	2.99	···	12	···
7		281 ± 24	0	281 ± 24	3.73	···	15	···
10		282 ± 25	18 ± 9	300	4.16	5.10	16	14
13		158 ± 24	81 ± 22	239	4.17	5.14	16	14
17		144 ± 25	236 ± 30	380	4.22	5.16	16	15
0	0.05	111 ± 4	0	111 ± 4	2.14	···	15	···
3		105 ± 9	0	105 ± 9	3.17	···	17	···
7		119 ± 10	0	119 ± 10	4.10	···	22	···
10		69 ± 6	30 ± 6	99	4.49	5.08	22	26
13		35 ± 5	54 ± 7	89 ± 8	4.44	5.23	16	25
17		18 ± 3	104 ± 9	122 ± 9	4.51	5.41	21	24

internal energy over translational energy. The net result of this is that for $H_2^+ + H_2$ at 0.5 eV, 95% of the available energy ends up as product internal energy.

The $\langle J \rangle$ values show a small increase between $v = 0$ and $v = 7$ and then are relatively constant for both S and M at higher v, with S and M values that are essentially the same. These results are consistent with the idea that H_3^+ rotation is mostly determined by kinematics, with a sizable portion of the reagent orbital angular momentum going to product rotation.

B. Cross sections for isotopic variants of $H_2^+ + H_2$

For the remainder of this paper we will consider just two vibrational states, $v = 13$ and 17, and one translational energy, 0.5 eV, in our analysis. These v's were chosen because they are representative of states which efficiently produce H_3^+ at or above its dissociation energy at both translational energies. As a result, they should be significant contributors to the H_3^+'s observed by Carrington and Kennedy. In considering reactions (3) and (4) where D_2^+ is involved, we used $v = 18$ and 24 as this leads to total energies which are almost the same as for $v = 13$ and 17, respectively, in H_2^+.

Table II presents cross sections for the four isotopic variants of $H_2^+ + H_2$ for the states indicated above. Simple Langevin theory predicts that the total cross section should be independent of isotope, and we see that the results in the table follow this prediction almost within statistical uncertainty. Likewise, the ratio of S to M cross sections is not strongly isotope dependent.

Now let us turn our attention to the metastable triatomic ion products produced in reactions (1)–(4). Table III presents the cross sections broken down into quasistable (Q), dissociating (D) and metastable (M) categories (with $M = D + Q$). "Dissociating" in this case refers to triatomics which live for at least 0.36 ps but dissociate within 30 ps. Note that the results are separately enumerated for the H_2D^+ and D_2H^+ products from reactions (3) and (4), thereby making it possible to determine isotopic branching ratios. Isotopic branching in the dissociating metastables is also given (with the labels "H^+" or "D^+" used). In addition, Table III gives $\langle E_{\text{int}} \rangle$ and $\langle J \rangle$ values for each of the product categories.

TABLE II. Cross sections for isotopic variants of $H_2^+ + H_2$ at $E_{\text{tr}} = 0.5$ eV.

	$Q(a_0^2)$		
Reaction	Stable (S)	Metastable (M)	Total (T)
H_2^+ (13) + H_2	35 ± 5	54 ± 7	89 ± 8
H_2^+ (13) + D_2	42 ± 5	60 ± 7	102 ± 8
D_2^+ (18) + H_2	43 ± 6	62 ± 7	106 ± 8
D_2^+ (18) + D_2	47 ± 6	57 ± 7	105 ± 8
H_2^+ (17) + H_2	18 ± 3	104 ± 9	122 ± 9
H_2^+ (17) + D_2	35 ± 5	90 ± 9	125 ± 9
D_2^+ (24) + H_2	23 ± 4	109 ± 10	133 ± 10
D_2^+ (24) + D_2	20 ± 4	101 ± 9	121 ± 9

Since there is a lot of information in Table III, let us itemize the important comparisons and conclusions.

(a) First, consider the branching of metastables between Q and D. Table III indicates that quasistables are very common for the lower v for each reaction, making up 21%–51% of the total metastable population (i.e., $Q/M = 0.21$–0.51), but they are less common for the higher v. Within statistical uncertainty, there is no significant variation of the Q/M ratio with reagent or product isotopic substitution.

(b) The branching between H^+ and D^+ formation in the dissociation of H_2D^+ and D_2H^+ shows one discernible trend. This is that H_2D^+ tends to dissociate to H^+ predominantly while D_2H^+ dissociates to D^+. The variation of the branching ratio with either v or with reagent isotopic substitution is not large enough to be statistically significant.

(c) The internal energies and angular momenta in Table III also show one important trend. For most isotopes, $\langle E_{\text{int}} \rangle$ is smaller and $\langle J \rangle$ is larger for the Q products than for D. Within the dissociating subgroup, the branching between H^+ and D^+ dissociation is not generally correlated with large differences in $\langle J \rangle$ or $\langle E_{\text{int}} \rangle$ values. However, an exception to this occurs in the dissociation of D_2H^+ from $D_2^+ + H_2$ where $\langle J \rangle$ is much higher for D^+ dissociation than H^+ dissociation. The underlying mechanisms for these results will be discussed in Secs. III D and IV.

(d) Finally, Table III shows that production of D_2H^+ is substantially favored over H_2D^+ in $H_2^+ + D_2$, but H_2D^+ is likewise favored in $D_2^+ + H_2$. This is consistent with the idea that the proton transfer mechanism[5(c)] for reaction is dominant over atom transfer for highly excited reagent ions. This is the sensible result given that a reagent ion should have the most easily cleaved bond. At the same time, the dominance of proton transfer over atom transfer contrasts strongly with the reaction mechanism for low v[5(c)] where both mechanisms are of comparable importance. Although it is not apparent that $\langle E_{\text{int}} \rangle$ varies much with which triatomic ion is formed, $\langle J \rangle$ is usually larger for H_2D^+.

C. Dissociation lifetimes

Figure 2 presents a semilog plot of survival probability vs time for the metastable triatomic ions produced in $H_2^+ + H_2$, including the subdivision of the results into dissociating and quasistable contributions. Initial time in this plot is determined by when the triatomic ion product has separated from the atom product by 16 a_0. Triatomic ions which dissociate within the first 0.36 ps are not included in the survival probability (thereby removing an initial transient which often occurs in decay plots[12]). The division into quasistable and dissociating populations is based on products found after 30 ps. Plots similar to Fig. 2 for the other isotopes have been omitted as they are all close in appearance to Fig. 2.

Although the curves in Fig. 2 are somewhat bumpy because of bad statistics, that associated with the dissociating population is roughly linear at short times (< 10 ps), implying simple unimolecular (exponential) behavior. Approximate lifetimes determined by visually fitting a straight line to

TABLE III. Cross sections, average product internal energies and rotational angular momenta for metastable[a] $H_2^+ + H_2$, and isotopic variants.

v	Final state	Cross Section	$\langle E_{int}$ (eV)$\rangle$	$\langle J \rangle$
		(A) $H_2^+ + H_2 \rightarrow H_3^+ + H$		
13	Dissociating (D) H^+	36 ± 6	5.31	23
	Quasistable (Q)	18 ± 5	5.08	29
	Metastable ($M = D + Q$)	54 ± 7	5.23	25
17	Dissociating H^+	98 ± 9	5.43	23
	Quasistable	6 ± 3	5.04	29
	Metastable	104 ± 9	5.41	24
		(B1) $H_2^+ + D_2 \rightarrow H_2D^+ + D$		
13	Dissociating H^+	10 ± 3	5.26	25
	D^+	1 ± 1	5.28	27
	Quasistable	10 ± 4	5.07	39
	Metastable	21 ± 5	5.17	32
17	Dissociating H^+	7 ± 2	5.38	29
	D^+	1 ± 1	5.10	21
	Quasistable	3 ± 2	5.08	34
	Metastable	11 ± 3	5.26	30
		(B2) $H_2^+ + D_2 \rightarrow D_2H^+ + H$		
13	Dissociating H^+	11 ± 4	5.18	27
	D^+	20 ± 5	5.19	23
	Quasistable	8 ± 3	5.03	30
	Metastable	39 ± 6	5.15	26
17	Dissociating H^+	20 ± 4	5.35	23
	D^+	56 ± 8	5.40	30
	Quasistable	3 ± 2	4.97	28
	Metastable	79 ± 9	5.37	28
		(C1) $D_2^+ + H_2 \rightarrow H_2D^+ + D$		
18	Dissociating H^+	14 ± 4	5.32	28
	D^+	13 ± 3	5.27	24
	Quasistable	12 ± 4	5.09	40
	Metastable	40 ± 6	5.24	31
24	Dissociating H^+	47 ± 8	5.45	29
	D^+	30 ± 7	5.52	38
	Quasistable	10 ± 3	5.12	33
	Metastable	86 ± 10	5.44	33
		(C2) $D_2^+ + H_2 \rightarrow D_2H^+ + H$		
18	Dissociating H^+	2 ± 1	5.22	14
	D^+	14 ± 4	5.23	27
	Quasistable	6 ± 2	5.00	23
	Metastable	22 ± 4	5.14	24
24	Dissociating H^+	5 ± 2	5.36	18
	D^+	13 ± 4	5.42	30
	Quasistable	5 ± 2	5.08	35
	Metastable	23 ± 5	5.33	28
		(D) $D_2^+ + D_2 \rightarrow D_3^+ + D$		
18	Dissociating D^+	38 ± 6	5.22	32
	Quasistable	20 ± 5	5.05	42
	Metastable	57 ± 7	5.16	36
24	Dissociating D^+	95 ± 9	5.38	33
	Quasistable	6 ± 2	5.13	41
	Metastable	101 ± 9	5.37	33

[a] Metastable results are subdivided into "Dissociating" and "Quasistable" contributions depending on whether or not dissociation occurs within 30 ps after formation.

this curve and to its counterparts for the other isotopes are all in the 2–7 ps range, with smaller values for the higher v for each reaction. Variations of these lifetimes with reagent or product isotope are generally within a factor of 2, which is within statistical uncertainty in most cases.

D. Analysis of product internal states

An important question concerning the quasistable triatomic ion products of reactions (1)–(4) is what is the nature of their vibrational and rotational motions. This question is

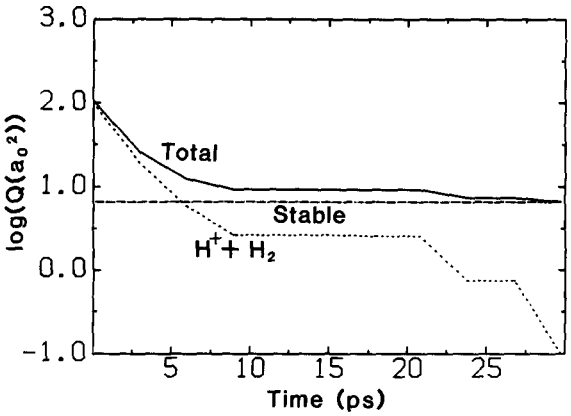

FIG. 2. Logarithm (base 10) of survival probability (expressed in terms of the $H_2^+ + H_2$ reactive cross section) vs time (ps) for H_3^+ metastables produced from H_2^+ ($v = 17$) + H_2. The curve labeled "total" (solid) is the sum of "dissociating" (dotted) and "quasistable" (dashed) contributions.

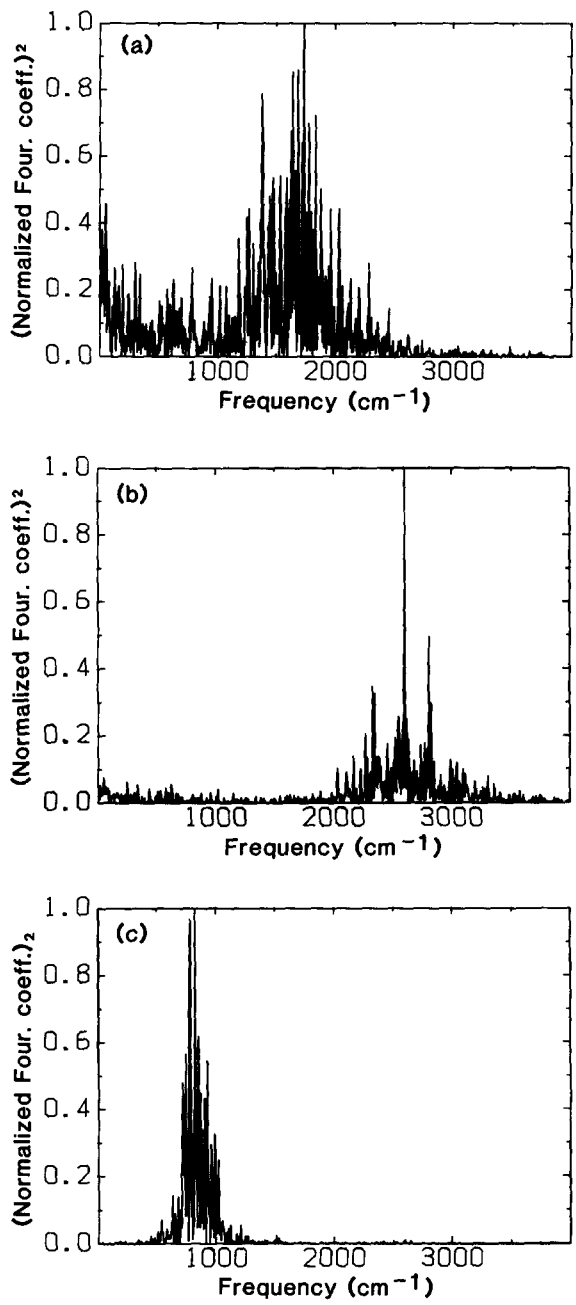

FIG. 3. Power spectrum associated with three H_3^+ coordinates: (a) R, (b) r, (c) orbital angular momentum. The H_3^+ in this case has $E_{int} = 5.32$ eV, $J = 32.4$, and is quasistable.

related to the origin of their quasistability, and in addition it is crucial to understanding the complex infrared absorption spectrum observed for these ions. Unfortunately, the characterization of classical motion for triatomic molecules moving in three dimensions is not straightforward.

During the course of this investigation we examined the triatomic motions in a variety of different ways. Movies were made of many trajectories to see if constraints on motion that would cause stability would be visually apparent. For essentially all the trajectories studied, the motion seemed to be chaotic except occasionally for short intervals. In no case did we encounter an H_3^+ that moved as a loosely coupled H_2–H^+ orbiting complex for more than a few H_2 vibrational periods, even for the highest J's. In most cases, whenever a H_2–H^+ complex was formed for a brief period, a hard collision between the H_2 and H^+ would quickly cause exchange of atoms between the H^+ and one of the two H's, leading to a new H_2–H^+ complex that would likewise live for only a brief period.

We also plotted trajectories in configuration and in phase space using coordinate projection and surface of section techniques developed by Hase and co-workers.[13] In all cases, chaotic behavior was observed except for brief intervals.

Another analysis was performed by examining power spectra of selected coordinates. Figure 3 presents the spectrum for a quasistable H_3^+ molecule in a state of relatively high angular momentum ($J = 32.4$) and which is above the rigorous barrier to dissociation. The three variables whose time evaluation was Fourier analyzed are (1) the H_2–H^+ intermolecular distance (R), (2) the corresponding H_2 internuclear distance (r), and (3) the orbital angular momentum (l) associated with the motion of H^+ about H_2. Whenever exchange of the three atoms occurred such that the identity of the H_2 fragment changed, the coordinates were redefined so that the H_2 fragment always had the smallest vibrational action of any of the diatomic pairs in the H_3^+. Figures 3(a) and 3(b) show that the peaks corresponding to R motions at 1200–2200 cm^{-1} and r motions at 2200–3200 cm^{-1} are very broad, with widths of 1000 cm^{-1} or more. This is characteristic of extreme chaos in which regular motion rarely persists for more than a vibrational period. However, the peak at 800 cm^{-1} in Fig. 3(c) associated with orbital motion is much narrower, indicating that this type of motion is closer to being regular. The power spectra of quasistable trajectories which are bound by rigorous centrifugal barriers are not significantly different from those in Fig. 3.

From the above results we conclude that few if any of the quasistable triatomics are quasiperiodic, and thus that the determination of action variables and semiclassical eigenvalues is not possible. At the same time, however, there is some indication that orbital motion of the H_2–H^+ com-

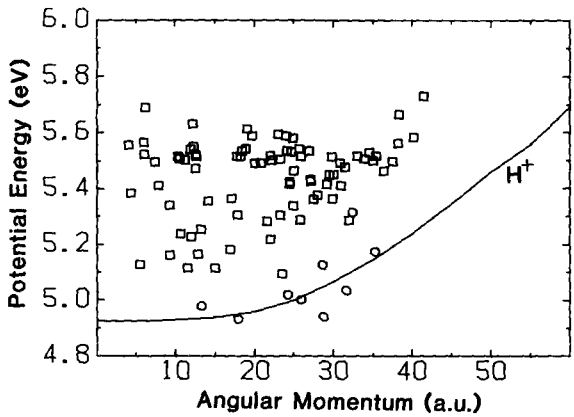

FIG. 4. E_{int} vs J for H_3^+ products from H_2^+ ($v = 17$) + H_2 at 0.5 eV translational energy, with squares denoting dissociating and circles quasistable H_2^+'s. Centrifugal barrier from Fig. 1 is superimposed.

plex is constrained, even for molecules that are not bound by centrifugal barriers, so let us now see if quasistability can be correlated with this. To study this, E_{int}–J values obtained from each of our trajectories have been superimposed with the centrifugal barriers taken from Fig. 1, yielding Fig. 4 for $H_2^+ + H_2$ and similar plots (not shown) for the other isotopes. The outcome of every metastable trajectory is indicated, with quasistable products denoted by circles and dissociating products by squares.

An examination of Fig. 4 reveals that many of the trajectories that are classified as quasistable are below the centrifugal barrier. However, we also find some molecules that are quasistable even though they are above (usually just slightly above) this barrier. This is also found for the other isotopes. Thus it appears that intramolecular randomization is slow enough for molecules that are above but close to one or both of the centrifugal barriers to make them stable for at least 30 ps. Presumably this slowness is due to the partial decoupling of orbital and rotational motion that was noted in analyzing Fig. 3.

Figures 1 and 4 can also be used to explain some of the results that we noted earlier in discussing Table III. For example, we found that the $\langle J \rangle$'s for quasistable products were always higher than for dissociating products. This is now seen to be a natural consequence of the fact that E_b is higher for higher J and this also leads to lower $\langle E_{int} \rangle$'s for the quasistables. The variation of the Q/M ratio with increasing v involves moving the E_{int} distribution up in Fig. 4 while keeping $\langle J \rangle$ constant (as noted in Tables I and III) and thus it makes sense that Q/M decreases as noted in Sec. III B. At the same time the rather weak dependence of the Q/M ratio on isotope is the result of cancellation between two effects. If we compare $H_2^+ + H_2$ with $D_2^+ + D_2$, for example, we note in Fig. 1 that for a given J, the $D_2^+ + D_2$ barrier is lower so one would expect fewer D_3^+ quasistables. However, Table III shows that the D_3^+'s have higher angular momenta than the H_3^+'s and this occurs in such a way that the average effective centrifugal barrier is about the same. As a result the Q/M ratios are about the same.

IV. DISCUSSION OF EXPERIMENTS, CONCLUSION

Although the comparisons between our results and the experiments in Ref. 6 are very qualitative, a number of points can be made. First, the results in Tables I–III indicate that $H_2^+ + H_2$ is capable of producing highly excited H_3^+'s in copious amounts. In addition, a substantial fraction of these H_3^+'s are "quasistable," meaning that they have enough energy to dissociate but live for at least 30 ps. Although most of these quasistables have energies less than 0.5 eV above the dissociation threshold, it seems likely that higher energy quasistables are produced. However, as noted by Pollak,[10] there are limits as to how high the energy can be if the H_3^+'s are to be centrifugally bound.

It is not feasible for us to simulate H_3^+ motions on a time scale that is relevant to the experiments ($> 10^{-7}$–10^{-9}s), and even if we could, we would not be able to determine lifetime distributions for centrifugally bound quasistables as these are determined by tunneling. We are, however, able to make a few conclusions concerning the nature of H_3^+ vibration/rotation motions that occur for these long-lived quasistables. In particular we find that the quasistables are not weakly coupled H_2–H^+ orbiting complexes. Instead, we find chaotic vibrational motion which is characterized by strong collisions between the three atoms that leads to rapid exchange between loosely and strongly bound atoms in the H_3^+. Despite this, many quasistable molecules are found to have energies that are above any rigorous centrifugal barrier, suggesting that partial decoupling of orbital and rotational motions inhibits vibrational redistribution that would lead to dissociation. This conclusion is closely related to Child's result[9] that the longest lived states are bound behind the $l = J$ or $l = J - 1$ centrifugal barrier. Unfortunately, chaotic vibrational motion causes our H_3^+ spectra to have rather broad features, so we are unable to make specific comments concerning the detailed absorption spectra that would be associated with the long lived H_3^+'s. However, we can say that none of the H_3^+'s that we studied would have the H_2 free rotor spectrum that Carrington and Kennedy used to interpret their results.

Although Ref. 6 did study H_2D^+ and D_2H^+ starting from mixtures of H_2 and D_2, the analysis was less detailed, and few of the conclusions in that paper can be compared with our results. Perhaps the most interesting result of Ref. 6 was that the spectra of D_2H^+ measured by monitoring H^+ are different than those taken monitoring D^+. This suggests that nearby predissociative states can have very different dissociation branching ratios. In addition, it was found that photodissociation of D_2H^+ to give H^+ was three times more intense than photodissociation to D^+. Since these conclusions refer to the dissociation of D_2H^+ following the absorption of one photon, they are not directly related to what we have calculated. However, our analysis does indicate that the centrifugal barriers play an important role in determining dissociation behavior, so it is interesting to see what predictions would be made assuming that photoabsorption by a quasistable molecule increases E_{int} but not J, thereby shifting molecules from below to above a centrifugal barrier. Figure 1 indicates that the centrifugal barrier for $D_2H^+ \rightarrow D^+$

$+ HD$ is always lower than for $D_2H^+ \rightarrow H^+ + D_2$, suggesting that dissociation to D^+ should be favored, just the opposite of what was measured. However this analysis ignores the possibility that different states of D_2H^+ might be "predestined" to dissociate in a specific way. One way to see if this is happening is to compare dissociation branching ratios for D_2H^+ formed by $H_2^+ + D_2$ and $D_2^+ + H_2$. Table III indicates that these ratios are *not* very different which argues against "predestination." However the ratio in Table III refers to D_2H^+'s that dissociate within the first few picoseconds, which are not the molecules that were seen in Ref. 6.

ACKNOWLEDGMENT

This research was supported by a grant from the National Science Foundation (CHE-8416026).

[1]A. J. Dempster, Philos. Mag. **31**, 438 (1916), and references therein.
[2]S. L. Anderson, F. A. Houle, D. Gerlich, and Y. T. Lee, J. Chem. Phys. **75**, 2153 (1981), and references therein.
[3]L. R. Wright and R. F. Borkman, J. Chem. Phys. **77**, 1938 (1982), and references therein.
[4](a) R. Polak, Chem. Phys. **16**, 353 (1976); (b) L. Pederson and R. N. Porter, J. Chem. Phys. **47**, 4751 (1967); (c) J. R. Krenos, K. K. Lehmann, J. C. Tully, P. M. Hierl and G. P. Smith, Chem. Phys. **16**, 109 (1976); (d) J. R. Stine and J. T. Muckerman, J. Chem. Phys. **68**, 185 (1978).
[5](a) J. R. Stine and J. T. Muckerman, J. Chem. Phys. **65**, 3975 (1976); (b) J. T. Muckerman, Theor. Chem. **6**, 1, 1981; (c) C. W. Eaker and G. C. Schatz, J. Phys. Chem. **89**, 2612 (1985); (d) C. W. Eaker and J. L. Muzyka, Chem. Phys. Lett. **119**, 169 (1985); (e) C. W. Eaker and G. C. Schatz, *ibid.* **127**, 343 (1986).
[6]A. Carrington and R. A. Kennedy, J. Chem. Phys. **81**, 91 (1984).
[7]W. H. Miller and T. F. George, J. Chem. Phys. **56**, 5637 (1972).
[8]J. K. Badenhoop, G. C. Schatz, and C. W. Eaker, Int. J. Quantum Chem. Symp. **31**, 57 (1987).
[9]M. S. Child, J. Chem. Phys. **90**, 3595 (1986).
[10]E. Pollak, J. Chem. Phys. **86**, 1645 (1987).
[11]K. Reinefors and S. Nordholm, Chem. Phys. **95**, 345 (1985); W. J. Chesnavich, J. Chem. Phys. **77**, 2988 (1982).
[12]S. B. Woodruff and D. L. Thompson, J. Chem. Phys. **71**, 376 (1979); G. C. Schatz, V. Buch, M. A. Ratner and R. B. Gerber, *ibid.* **79**, 1808 (1983).
[13]R. J. Duchovic, K. N. Swamy, and W. L. Hase, J. Chem. Phys. **80**, 1462 (1984).